Orientations of Tyrosines 21 and 24 in Coat Subunits of *Ff* Filamentous Virus: Determination by Raman Linear Intensity Difference Spectroscopy and Implications for Subunit Packing

Motonori Matsuno,* Hideo Takeuchi,* Stacy A. Overman,# and George J. Thomas, Jr.#
*Pharmaceutical Institute, Tohoku University, Aobayama, Sendai 980-8578, Japan, and #Division of Cell Biology and Biophysics, School of Biological Sciences, University of Missouri–Kansas City, Kansas City, Missouri 64110 USA

ABSTRACT Virions of the *Ff* group of bacteriophages (*fd, f1, M13*) are morphologically identical filaments (~6-nm diameter × ~880-nm length) in which a covalently closed, single-stranded DNA genome is sheathed by ~2700 copies of a 50-residue α-helical subunit (pVIII). Orientations of pVIII tyrosines (Tyr^{21} and Tyr^{24}) with respect to the filament axis have been determined by Raman linear intensity difference (RLID) spectroscopy of flow-oriented mutant virions in which the tyrosines were independently mutated to methionine. The results show that the twofold axis of the phenolic ring (C1–C4 line) of Tyr^{21} is inclined at 39.5 ± 1.4° from the virion axis, and that of Tyr^{24} is inclined at 43.7 ± 0.6°. The orientation determined for the Tyr^{21} phenol ring is close to that of a structural model previously proposed on the basis of fiber x-ray diffraction results (Protein Data Bank, identification code 1IFJ). On the other hand, the orientation determined for the Tyr^{24} phenol ring differs from the diffraction-based model by a 40° rotation about the Cα-Cβ bond. The RLID results also indicate that each tyrosine mutation does not greatly affect the orientation of either the remaining tyrosine or single tryptophan (Trp^{26}) of pVIII. On the basis of these results, a refined model is proposed for the coat protein structure in *Ff*.

INTRODUCTION

Bacteriophages *fd*, *f1*, and *M13* belong to the *Ff* group of the class I filamentous viruses infecting F^+ strains of *Escherichia coli*. The *Ff* virion is a flexible filament with a length of ~880 nm and a diameter of ~6 nm. The filament contains a covalently closed and single-stranded (ss) DNA genome of 6410 nucleotides, which is covered by a protein sheath comprising ~2700 copies of a 50-residue α-helical protein subunit (pVIII), the product of viral gene VIII. The amino acid sequence of the pVIII subunit is identical among virions of the *Ff* class (^{1}AEGDDPAKAA FDSLQASATE YIGYAWAMVV VIVGATIGIK LFKKFTSKAS^{50}), except for the replacement of Asp by Asn at position 12 in *M13*. Further details of the molecular genetics and architecture of the *Ff* virus are given in the monograph edited by Denhardt et al. (1978) and in more recent reviews (Day et al., 1988; Webster, 1996).

The structure of the pVIII subunit in the *Ff* virion has been studied extensively by a variety of spectroscopic methods, including Raman spectroscopy (Thomas and Murphy, 1975; Thomas et al., 1983; Williams et al., 1984; Thomas, 1985; Aubrey and Thomas, 1991; Overman et al., 1994; Overman and Thomas, 1995), linear dichroism (Bendet and Mayfield, 1976; Fritzsche et al., 1981; Clack and Gray, 1992), circular dichroism (CD) (Clack and Gray, 1989; Arnold et al., 1992), and solid-state NMR spectroscopy (Opella et al., 1980, 1987; Cross et al., 1983; Cross and Opella, 1985). The body of spectroscopic work indicates that the pVIII subunit is a continuous α-helix tilted at a small (< 30°) angle with respect to the filament axis. Very recent polarized Raman measurements indicate that the average subunit tilt angle is ~16° (Overman et al., 1996). Fiber x-ray diffraction and model building studies show that the DNA core of *Ff* is coated by a helical array of pVIII subunits arranged with fivefold rotational symmetry and an approximately twofold screw axis (Marvin et al., 1974; Wachtel et al., 1974; Marvin and Wachtel, 1975, 1976; Banner et al., 1981; Makowski and Caspar, 1981; Marzec and Day, 1988; Bhattacharjee et al., 1992; Glucksman et al., 1992; Symmons et al., 1995; Williams et al., 1995). Although atomic details of the coat protein cannot be determined solely by fiber x-ray diffraction, Marvin (1990) proposed a molecular model for the pVIII assembly on the basis of the subunit arrangement revealed by fiber x-ray diffraction and available spectroscopic data, including atomic coordinates of a C-terminal (Lys^{40}–Phe^{45}) portion revealed by solid-state NMR spectroscopy (Cross and Opella, 1985). The model was later refined by energy minimization calculations and by taking into account additional fiber x-ray diffraction, Raman spectroscopic, and biochemical data (Marvin et al., 1994). Coordinates of the model are deposited in the Protein Data Bank, identification code 1IFJ (Symmons et al., 1995). The model is such that the acidic N-terminal region of the pVIII subunit is exposed to the surrounding solvent on the outer surface of the protein sheath, whereas the basic C-terminal region is located on the inner surface, interacting with the DNA core. The central region of the pVIII subunit, which is rich in hydrophobic

Received for publication 10 December 1997 and in final form 23 February 1998.

Address reprint requests to Dr. George J. Thomas, Jr., Division of Cell Biology and Biophysics, School of Biological Sciences, BSB 405, University of Missouri–Kansas City, 5100 Rockhill Rd., Kansas City, MO 64110. Tel.: 816-235-5247; Fax: 816-235-1503; E-mail: thomasgj@cctr.umkc.edu; or to Dr. Hideo Takeuchi, Pharmaceutical Institute, Tohoku University, Aobayama, Sendai, 980-8578, Japan.

0006-3495/98/06/3217/09 $2.00

residues and includes Tyr^{21}, Tyr^{24}, and Trp^{26}, is involved mainly in intersubunit interactions. Although the general features of this model seem reasonable, the details of the virion architecture, in particular the conformations and interactions of side chains, need to be tested experimentally.

Recently we established Raman linear intensity difference (RLID) spectroscopy of flow-oriented macromolecules and their assemblies as a practical method for evaluating residue orientations in filamentous viruses (Takeuchi et al., 1996). Particles like the filamentous viruses can be aligned by hydrodynamic shear force in a flow cell, and the orientation of a chromophore in the aligned particle can be determined from the resonance Raman spectral intensities excited with laser polarizations alternatively parallel and perpendicular to the direction of filament alignment. For *Ff* viruses, the aromatic amino acid side chains of pVIII subunits are particularly appropriate chromophores for RLID analysis when UV laser excitation is employed. By exploiting the fact that pVIII contains a single tryptophan (Trp^{26}), the indole ring orientation in the *fd* virion was determined by RLID analysis (Takeuchi et al., 1996). In the RLID determination, the indole ring plane is inclined at 31 ± 4° from the virion axis, and its pseudo-twofold axis makes an angle of 38 ± 6° with the virion axis. The salient features of the Trp^{26} indole ring orientation have been confirmed independently by off-resonance polarized Raman microspectroscopic measurements on oriented *fd* fibers (Tsuboi et al., 1996a), making use of previously determined Raman tensors of the indole moiety (Tsuboi et al., 1996b). The Trp^{26} ring orientation proposed in the model of Marvin and coworkers is not entirely consistent with the experimentally determined orientation. Although the indole plane is close to parallel to the virion axis in the diffraction-based model, it requires an ~180° flip about the Cβ-C3 linkage to achieve compatibility with the RLID and polarized Raman experimental results.

In this study we have applied RLID spectroscopy to the tyrosine residues, Tyr^{21} and Tyr^{24}, of the pVIII subunit in *Ff*. To distinguish the two tyrosines, we have examined single-site mutants of the *f1* strain, *f1*(Y21M) and *f1*(Y24M), in which the indicated tyrosine residue is replaced by methionine. Use of the single-site mutants enabled determination of the orientation of the phenolic twofold axis with respect to the virion axis for both Tyr^{21} and Tyr^{24}. The RLID results show that the phenolic twofold axes of Tyr^{21} and Tyr^{24} are inclined, respectively, at angles of 39.5 ± 1.4° and 43.7 ± 0.6°. Whereas the orientation of Tyr^{21} measured by RLID is close to that of the diffraction-based model (Marvin et al., 1994; Symmons et al., 1995), the present analysis shows that a rotation of 40° about the Cα-Cβ bond is required for Tyr^{24}. This relatively large adjustment, together with the above-noted need for an ~180° flip of the Trp^{26} indole ring, produces a dramatic change in intersubunit hydrogen-bonding possibilities in the *Ff* assembly. We propose a revised model for the coat protein structure in the *Ff* virion and show that plausible hydrogen bonding states of Tyr^{21}, Tyr^{24}, and Trp^{26} in this revised model are consistent with those deduced from Raman marker bands of phenolic and indole hydrogen bonding.

MATERIALS AND METHODS

Mutant phages, *f1*(Y21M) and *f1*(Y24M), were the gift of Prof. Gianni Cesareni (Dipartimento di Biologia, Università di Roma, Rome). The methods of preparation and purification of the phages have been described (Overman et al., 1994). Briefly, the phages were grown in MS media with *Escherichia coli* strain Hfr3300 as host. Mature viral particles, extruded through the bacterial membrane into the growth media, were collected by poly(ethylene glycol) precipitation followed by low-speed centrifugation. The phage particles were purified either on a continuous KBr gradient or by differential centrifugation. Repeated cycles of differential centrifugation in 10 mM Tris (pH 7.8) yielded a pellet from which samples were prepared for spectroscopic examination. The samples for Raman measurements were diluted with a buffer of 10 mM Tris (pH 7.8) to a concentration of ~1 mg/ml.

Flow orientation of phage particles was achieved using a Couette-type flow cell. Approximately 120 μl of virus solution was placed in the annular gap (0.5 mm) between the rotating outer cylinder (8.0-mm inner diameter) and the stationary inner rod (7.0-mm outer diameter) of the flow cell. To generate a velocity gradient (G) in the gap, the outer cylinder was rotated at 800 ($G = 670\ s^{-1}$), 1200 (1005), 1600 (1340), 2500 (2094), or 3600 rpm (3016). Raman spectra of flow-oriented phages were excited at 240 nm, using a pulsed Nd:YAG laser operating at a 30-Hz repetition rate. The 1064-nm pulses from the laser were frequency-quadrupled to generate radiation at 266 nm, which was then converted to 240 nm (~1 mW) by a hydrogen gas Raman shifter. Raman spectra were recorded in the 180° back-scattering geometry as described previously (Takeuchi et al., 1996). The Raman photons from the sample were collected with Cassegrain optics, dispersed by a double monochromator (Jasco CT-80D), and detected by an intensified diode array (Princeton Instruments D/SIDA-700IG). A pair of Raman spectra were recorded for each fresh sample with laser polarizations parallel and perpendicular to the flow orientation direction. The Raman band of H_2O near 3400 cm^{-1} was used as an internal intensity standard to correct for any small instrumental bias in intensity measurements. The spectra reported here are the averages of those recorded on six to nine identical samples.

The polarized and depolarized Raman spectra of aqueous L-tyrosine (1 mM) were recorded on the same Raman spectrometer as described above by using a conventional spinning cell and a Polacoat polarization analyzer.

RESULTS

Tyrosine Raman band amenable to RLID analysis

The principle of RLID spectroscopy and its experimental and theoretical aspects have been described in detail (Takeuchi et al., 1996). The Raman band to be used for RLID analysis must fulfill the requirement that the band is enhanced by a nondegenerate A-term resonance mechanism, so that the Raman tensor consists of a single nonzero diagonal element (Takeuchi et al., 1996). Experimentally, this requirement is tested by measuring the Raman depolarization ratio ρ of randomly oriented molecules. If the value of ρ is close to 1/3, the band can be regarded as arising from only one diagonal element of the Raman tensor. Fig. 1 *a* shows the UV absorption spectrum of the amino acid tyrosine in aqueous solution. The L_a electronic transition of tyrosine at 222 nm is polarized along the twofold axis of the phenolic ring, and the Raman vibrational bands that appear in Raman spectra excited at 240 nm are expected to gain

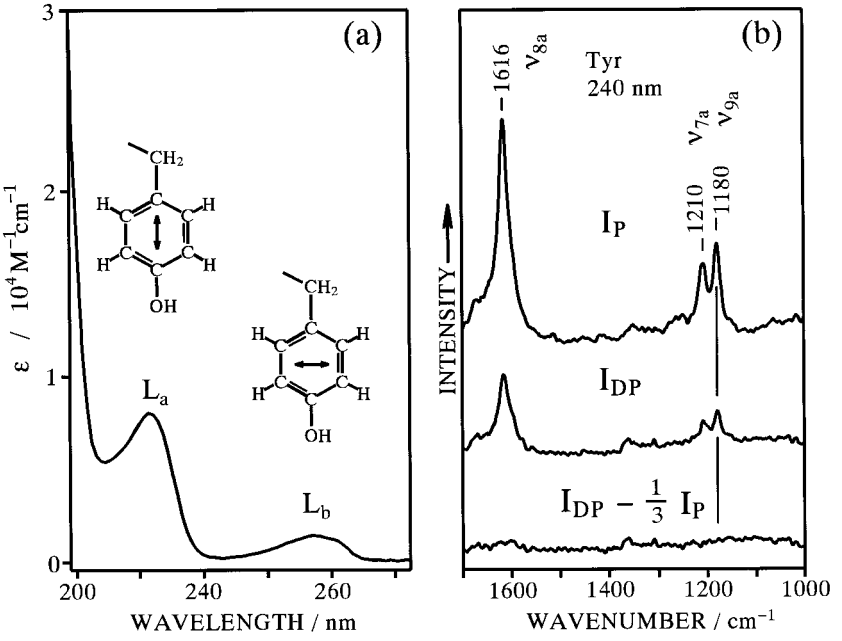

FIGURE 1 UV absorption (*a*) and UV resonance Raman (*b*) spectra of aqueous L-tyrosine at pH 7. The Raman spectra were excited at 240 nm for a 1 mM solution. I_P and I_{DP} denote polarized and depolarized Raman spectra, respectively. The bands that disappear in the difference $I_{DP} - I_P/3$ spectrum have depolarization ratios, ρ, close to 1/3.

intensity through resonance with the L_a transition. Fig. 1 *b* shows the polarized (I_P, *top trace*) and depolarized (I_{DP}, *middle trace*) Raman spectra of aqueous tyrosine excited at 240 nm, and their corresponding difference spectrum ($I_{DP} - I_P/3$, *bottom trace*). The intense I_P Raman band at 1180 cm^{-1}, denoted ν_{9a} (also referred to as normal mode Y9a), exhibits $\rho = 0.35 \pm 0.04$, indicating that this band is enhanced via A-term resonance with the L_a transition, and the predominant contributor of the Raman tensor is the diagonal element corresponding to the twofold axis direction. Raman bands at 1616 (ν_{8a}) and 1210 cm^{-1} (ν_{7a}) also show ρ values close to 1/3, but they cannot be used for RLID analysis of the *Ff* coat protein, because they are overlapped by tryptophan Raman bands (Takeuchi et al., 1996). Excitation at a longer wavelength, i.e., closer to the L_b transition (~260 nm), causes predominant resonance enhancement of tryptophan Raman bands, and the tyrosine Raman bands become almost undetectable. Accordingly, we have monitored the direction of the twofold axis of tyrosine through the Raman intensity of the ν_{9a} band in ultraviolet resonance Raman (UVRR) spectra excited at 240 nm.

Raman spectra of flow-oriented mutant virions, *f1*(Y21M) and *f1*(Y24M)

Fig. 2 shows Raman spectra of the mutant *f1*(Y21M) excited at 240 nm. The virus sample is oriented in a flow cell consisting of a rotating outer cylinder and a stationary inner rod separated by a thin annular gap (Takeuchi et al., 1996). The aqueous solution of *f1*(Y21M) is injected into the gap, and the flow velocity gradient (G) between the inner surface of the rotating cylinder and the outer surface of the stationary rod is kept constant at 3016 s^{-1}. Under such hydrodynamic shear force, the virion axes are expected to be largely aligned along the flow direction. The upper and middle traces in Fig. 2 were obtained, respectively, with laser polarizations parallel ($I_\parallel$) and perpendicular ($I_\perp$) to the flow direction. (The intensities of the spectra were normalized using the H_2O Raman band near 3400 cm^{-1} as an internal intensity standard.) The bottom trace shows the intensity difference $I_\parallel - I_\perp$. With 240-nm excitation, only tyrosine and tryptophan give prominent Raman bands. Raman bands

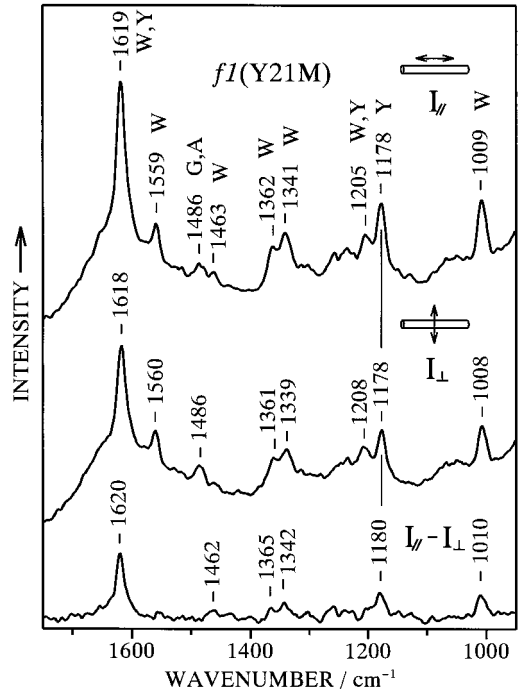

FIGURE 2 Resonance Raman spectra of flow-oriented *f1*(Y21M) virus (~1 mg/ml in 10 mM Tris) excited at 240 nm. The laser polarization is parallel ($I_\parallel$, *top*) or perpendicular ($I_\perp$, *middle*) to the axis of alignment. Also shown is the Raman linear intensity difference ($I_\parallel - I_\perp$, *bottom*).

of phenylalanine and of all nonaromatic residues are not significantly enhanced with 240-nm excitation. Similarly, Raman bands of the packaged DNA, which constitutes only ~12% of the total virion mass, are very weak, because of the excitation wavelength employed, as well as the fact that the bands are subject to very large hypochromic effects (Wen et al., 1997). Specific Raman band assignments to subunit tyrosines or tryptophan and genomic guanine or adenine residues are indicated in Fig. 2 by the labels Y, W, G, and A, respectively, in accordance with previous work (Takeuchi et al., 1996; Overman and Thomas, 1995; Wen et al., 1997). Because Tyr^{21} is replaced by methionine in the mutant *f1*(Y21M), the Raman bands labeled with Y are contributed exclusively by Tyr^{24}. The intense band at 1178 cm^{-1} is therefore ascribed to ν_{9a} of Tyr^{24}, enhanced by A-term resonance with the L_a transition. This Raman band is stronger in the $I_\parallel$ spectrum than in the $I_\perp$ spectrum, indicating that the laser polarization parallel to the virion axis produces larger resonance enhancement than does the perpendicular polarization. Thus the direction of the L_a transition moment (twofold axis) of Tyr^{24} is closer to the virion axis than to its normal. (Note that the intensity difference would be zero at the magic angle of 52° (Takeuchi et al., 1996).)

Fig. 3 shows the 240-nm polarized Raman spectra ($I_\parallel$, $I_\perp$, and $I_\parallel - I_\perp$) of the mutant *f1*(Y24M) oriented in the flow cell at the same velocity gradient ($G = 3016\ s^{-1}$) used for *f1*(Y21M). In these spectra, the tyrosine Raman bands arise exclusively from Tyr^{21}. As in the case of Fig. 2, the ν_{9a} Raman band of Tyr^{21} at 1178 cm^{-1} in Fig. 3 is stronger in the $I_\parallel$ spectrum than in the $I_\perp$ spectrum, so that the difference spectrum exhibits a positive peak. Therefore, the twofold axis of Tyr^{21} must also be directed close to the virion axis.

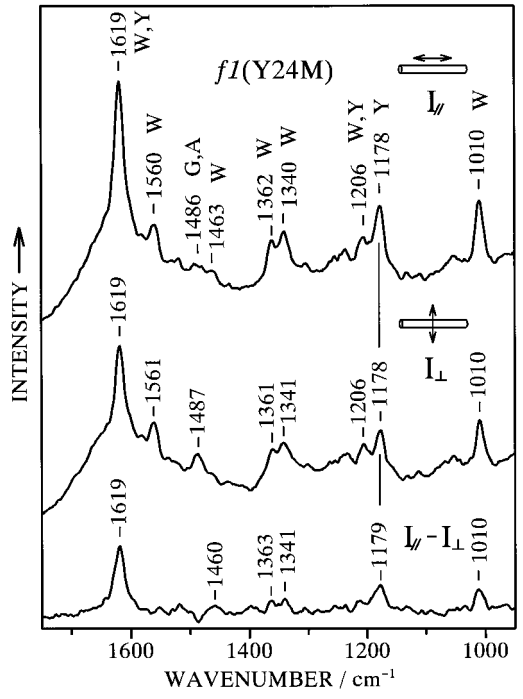

FIGURE 3 Resonance Raman spectra of flow-oriented *f1*(Y24M) virus (~1 mg/ml in 10 mM Tris) excited at 240 nm. The laser polarization is parallel ($I_\parallel$, *top*) or perpendicular ($I_\perp$, *middle*) to the axis of alignment. Also shown is the Raman linear intensity difference ($I_\parallel - I_\perp$, *bottom*).

Angle of inclination of the phenolic twofold axis in Tyr^{21} and Tyr^{24}

To obtain a precise value for the inclination angle of a transition moment in a filamentous particle, the Raman intensity difference for a perfectly aligned ensemble of particles must be known. However, the flow orientation method cannot achieve perfect alignment, because of rotational diffusion effects. Accordingly, the Raman intensity difference for perfect alignment is estimated from values measured at finite velocity gradients. As shown previously (Takeuchi et al., 1996), the degree of alignment increases linearly with decreasing $G^{-0.28}$. The reduced RLID, γ, defined by Eq. 1, is also a linear function of $G^{-0.28}$:

$$\gamma = \frac{3(I_\parallel - I_\perp)}{I_\parallel + 2I_\perp} \tag{1}$$

Thus the value of γ for perfect alignment can be estimated from experimental values at finite G by linear extrapolation. The value of γ so obtained is then related by Eq. 2 to the angle of inclination (ψ) of the chromophore transition moment with respect to the direction of alignment (in this case, the angle between the L_a transition moment of tyrosine and the filament axis; Takeuchi et al., 1996):

$$\gamma = \frac{3(5\cos^4\psi + 6\cos^2\psi - 3)}{2(\cos^4\psi + 3)} \tag{2}$$

We have also made RLID measurements at lower velocity gradients (G = 670, 1005, 1340, and 2094 s^{-1}). The values of γ obtained for the ν_{9a} bands of Tyr^{21} and Tyr^{24} at the lower velocity gradients, together with those at G = 3016 s^{-1}, are plotted against $G^{-0.28}$ in Fig. 4. Extrapolation to infinite G (i.e., $G^{-0.28} = 0$) gives $\gamma = 1.05 \pm 0.12$ for Tyr^{21} and 0.69 ± 0.05 for Tyr^{24}. These γ values correspond to completely aligned virions. By either Eq. 2 or the graphical γ-ψ relationship shown in the inset to Fig. 4, we obtain the following inclination angles of the phenolic twofold axes: $39.5 \pm 1.4°$ for Tyr^{21} and $43.7 \pm 0.6°$ for Tyr^{24}. It should be noted that the linear extrapolations of Fig. 4 are based on the assumption of nonturbulent flow of an infinitesimally thin filament (shape parameter, $r = (p^2 - 1)/(p^2 + 1) \cong 1$, where p is the axial ratio of the long and short axes of the filament) (Takeuchi et al., 1996). This approximation is appropriate to the present experiments, given the relatively low velocity gradients ($G < 4000\ s^{-1}$) employed and the dimensions of the *Ff* filament (~6 × ~880 nm, with $r \approx 0.9996$). Furthermore, as indicated in the inset to Fig. 4, the inclination angle ψ is not highly sensitive to γ in the region $-0.5 < \gamma < 1.5$. Accordingly, the inclination angles obtained for the L_a transition moments of Tyr^{21} and

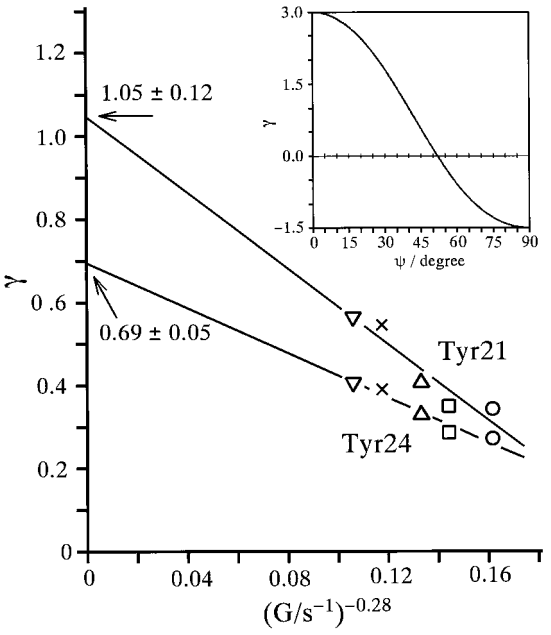

FIGURE 4 Plots of the reduced Raman linear intensity difference (γ) of the ν_{9a} band of Tyr^{21} and Tyr^{24} against $G^{-0.28}$, where G is the velocity gradient. Data for Tyr^{21} and Tyr^{24} were obtained from Raman spectra of *f1*(Y24M) and *f1*(Y21M), respectively. The straight lines represent least-squares fits of the data. The inset illustrates the relationship between γ and the inclination angle ψ, which are related by Eq. 2.

Tyr^{24} are not subject to large errors, even though a relatively long linear extrapolation is carried out in Fig. 4.

The inclination angles obtained here for Tyr^{21} and Tyr^{24} by using the *f1* mutants are consistent with the average inclination angle (41.2 ± 0.9°) for Tyr^{21} and Tyr^{24} obtained previously by RLID analysis on wild-type *fd* (Takeuchi et al., 1996). This consistency indicates that the mutation of either Tyr^{21} or Tyr^{24} to methionine does not significantly affect the orientation of the nonmutated tyrosine.

To examine the effects of tyrosine mutations on the orientation of Trp^{26}, we also determined the inclination angle of the indole ring B_b transition moment in *f1*(Y21M) and *f1*(Y24M) from γ values measured for the 1010 cm^{-1} Raman band (Figs. 2 and 3). As shown previously, the 1010 cm^{-1} band arises from an indole ring vibration that is enhanced via A-term resonance with the B_b transition at 218 nm (Takeuchi et al., 1996). The inclination angle obtained for the B_b transition moment of Trp^{26} is 46.2 ± 0.5° in *f1*(Y21M) and 45.7 ± 0.7° in *f1*(Y24M). Both inclination angles are within experimental error of the value (45.3 ± 1.1°) obtained for wild-type *fd* (Takeuchi et al., 1996). The orientation of the B_b transition moment, which is directed nearly parallel to the pseudo-twofold axis of the indole ring, is thus not significantly affected by the tyrosine mutations. This observation suggests that each single-site tyrosine mutation does not significantly alter the orientation of Trp^{26}. It is of interest to note, however, that off-resonance Raman spectra of *f1*(Y21M) and *f1*(Y24M) exhibit small but significant differences in Raman markers of their respective Trp^{26} residues, implying that the indole ring environments are not identical in the two cases (Overman and Thomas, 1995). The different Trp^{26} environments in *f1*(Y21M) and *f1*(Y24M) apparently do not result from different indole orientations with respect to the virion axis, but from different near-neighbor interactions, as further discussed below.

DISCUSSION

Modeling tyrosine and tryptophan orientations in *Ff*

Residues Tyr^{21}, Tyr^{24}, and Trp^{26} are located near the center of the 50-residue pVIII subunit, a region that is thought to play an important role in intersubunit packing (Marvin et al., 1994). The most detailed molecular model of intersubunit packing is the fiber diffraction-based model of Marvin and co-workers (Marvin et al., 1994; Symmons et al., 1995), the coordinates of which are deposited in the Protein Data Bank (identification code 1IFJ, hereafter referred to as model 1IFJ). Fig. 5 *a* illustrates subunit residues Tyr^{21}, Tyr^{24}, and Trp^{26} in relation to proximate residues of neighboring subunits in the 1IFJ model. In Fig. 5 *a*, the view is from the outside of the protein sheath toward the virion axis, and each subunit is indexed by an integer, k. Five subunits (e.g., $k = 0, 1, 2, 3, 4$) are arranged with fivefold rotational symmetry at the same axial position. Each such group is related to the next by a translation of 16.5 Å and rotation of −36.00° with respect to the virion axis. The 1IFJ model allows a hydrogen bond between the phenolic OH group of Tyr^{21} in the $k = 0$ subunit and the indole NH group of Trp^{26} in the $k = 5$ subunit (or, equivalently, between Tyr^{21} in the $k = -5$ subunit and Trp^{26} in the $k = 0$ subunit, as shown in Fig. 5 *a*). Another possible hydrogen bond involving tyrosine can occur between the phenoxyl OH donor of Tyr^{24} in the $k = 0$ subunit and the Oδ2 acceptor atom of an aspartate (Asp^{12}) in the $k = -6$ subunit. The twofold axes of both Tyr^{21} and Tyr^{24} in 1IFJ are inclined at 46° and 74°, respectively, from the virion axis. Thus the inclination angle of Tyr^{21} in the 1IFJ model is close to the value of 39.5 ± 1.4° that is determined by RLID spectroscopy, whereas that of Tyr^{24} deviates significantly from the experimental value of 43.7 ± 0.6°. The indole ring orientation of Trp^{26} in Fig. 5 *a* also differs greatly from the previously determined RLID and polarized Raman results (Takeuchi et al., 1996; Tsuboi et al., 1996a).

A refined *Ff* model based on the present RLID results

We have attempted to modify the 1IFJ model to incorporate the presently determined side-chain orientations for Tyr^{21} and Tyr^{24}, as well as the previously determined orientation for Trp^{26}. The modified model is shown in Fig. 5 *b*. A very similar model was obtained by modifying the 1IFI model that was proposed for the coat protein assembly with canonical symmetry (Marvin et al., 1994). The specific mod-

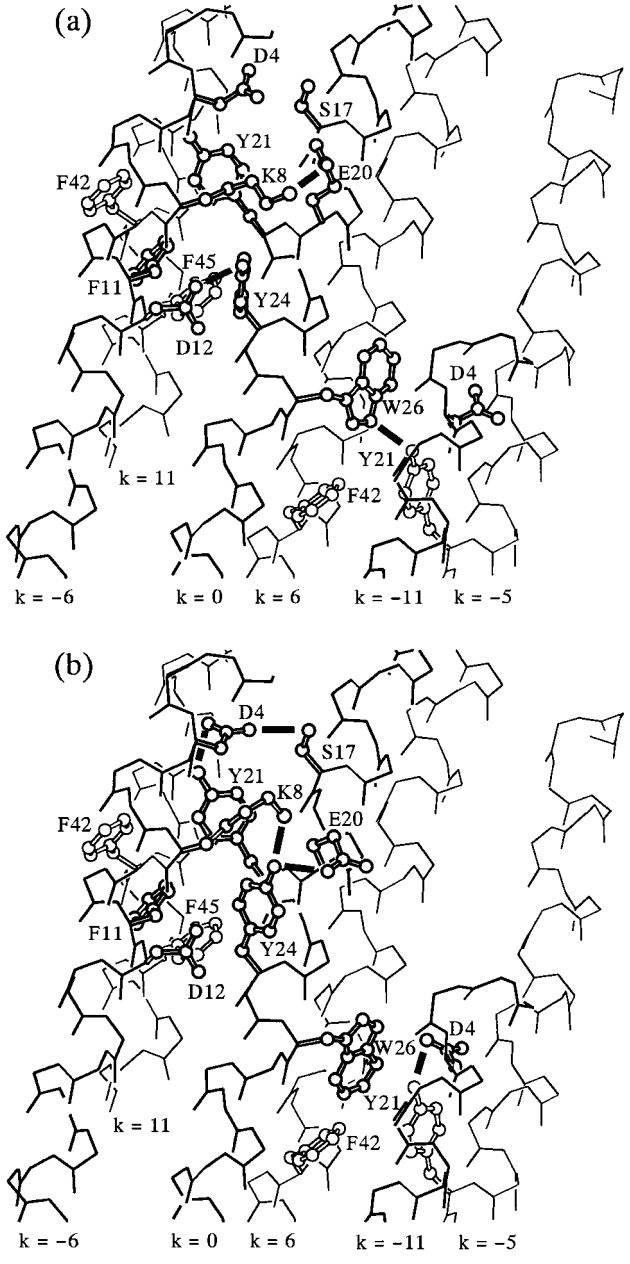

FIGURE 5 Orientations of Tyr^{21}, Tyr^{24}, and Trp^{26} side chains and intersubunit interactions in their vicinity. (*a*) Model proposed by Marvin and co-workers (Marvin et al., 1994; Symmons et al., 1995; Protein Data Bank, identification code 1IFJ). (*b*) Model proposed in this study. The view is from the outside of the virion toward the virion axis. The central subunit ($k = 0$) and five neighboring subunits ($k = -11, -6, -5, 6$, and 11) are shown. All side chains except those labeled are omitted for clarity. Possible hydrogen bonds are indicated with thick bars.

ifications include changes in the tyrosine χ^1 torsion angle (about the Cα-Cβ bond) from $-74°$ to $-69°$ for Tyr^{21} and from $-79°$ to $-39°$ for Tyr^{24}. Although the modified χ^1 value ($-39°$) for Tyr^{24} is small for a tyrosine residue in an α-helix (McGregor et al., 1987), it could be accommodated by relatively small changes in the structure of the main-chain α-helix or by changes in helix/main-chain torsion angles in the vicinity of Tyr^{24}. The χ^2 torsion angles (about the Cβ-Cγ bond) are assumed to be 90° and 150° for Tyr^{21} and Tyr^{24}, respectively, to avoid steric clash of the phenol ring with the helix main chain.

For the indole ring of Trp^{26}, the χ^1 torsion (about the Cα-Cβ bond) is increased in Fig. 5 *b* from the value of $-115°$ in 1IFJ (Fig. 5 *a*), in accordance with previous polarized Raman, molecular modeling, and energy minimization studies (Takeuchi et al., 1996; Tsuboi et al., 1996a). The indole $\chi^{2,1}$ torsion (about Cβ-C3) is kept in the range of $120 \pm 10°$, as required by the Raman marker band at 1560 cm^{-1} (Miura et al., 1989; Aubrey and Thomas, 1991; Takeuchi et al., 1996). In Fig. 5 *b*, we use 127°, which avoids close contacts with nearby groups (see below).

With the revised orientations for Tyr^{21} and Tyr^{24} in Fig. 5 *b*, it is clear that a hydrogen bond cannot occur between the phenolic OH group of Tyr^{21} and the indole NH of Trp^{26}. Nor can the OH donor group of Tyr^{24} form a hydrogen bond with the Asp^{12} acceptor. On the other hand, the model of Fig. 5 *b* would allow a hydrogen bond between the phenolic OH donor of Tyr^{21} ($k = 0$) and the Oδ2 acceptor of Asp^4 ($k = -6$). This requires χ^1 and χ^2 torsions of $-40°$ and 155°, respectively, for the Asp^4 side chain, which differs from the corresponding values of 44° and 87° in the 1IFJ model. It is interesting to note that this conformational modification introduces the possibility of an additional hydrogen bond (Fig. 5) between the Oδ1 acceptor of Asp^4 ($k = -6$) and a serine hydroxyl donor (Ser^{17}, $k = 0$) that is not otherwise hydrogen-bonded in the 1IFJ model.

For Tyr^{24}, there are two residues with which hydrogen bonds can be formed. Both glutamic acid (Glu^{20}, $k = 0$) and lysine (Lys^8, $k = -6$) could undergo hydrogen bonding with the Tyr^{24} phenolic group ($k = 0$). Such a Lys^8-Tyr^{24}-Glu^{20} linkage would require Lys^8 side-chain torsions of $\chi^1 = -60°$, $\chi^2 = 160°$, $\chi^3 = 170°$, and $\chi^4 = -60°$, and Glu^{20} torsions of $\chi^1 = -85°$, $\chi^2 = -55°$, and $\chi^3 = -65°$, supplanting the corresponding values of $-78°$, 179°, 63°, 178° for Lys^8 and $-67°$, 176°, $-66°$ for Glu^{20} of the 1IFJ model. Thus the salt bridge shown between Glu^{20} and Lys^8 in Fig. 5 *a* is replaced by the proposed Lys^8-Tyr^{24}-Glu^{20} hydrogen bonding scheme of Fig. 5 *b*.

Raman markers of tyrosine environments in filamentous viruses

Certain Raman bands of tyrosine are known to be sensitive in intensity or frequency (cm^{-1}) to the hydrogen bonding state of the phenolic OH group. A well-studied example is the pair of Raman markers (Fermi doublet) near 850 and 830 cm^{-1}, the relative intensity ratio of which (I_{850}/I_{830}) has been correlated with the state of phenolic hydrogen bonding in globular proteins (Siamwiza et al., 1975). The doublet arises from Fermi resonance involving the ring breathing fundamental vibration (expected near 840 cm^{-1}) and the first overtone of an out-of-plane ring bending vibration near 420 cm^{-1}. Values for I_{850}/I_{830} in globular proteins and in *para*-phenoxyl model compounds typically range between

0.3 (when OH is a strong hydrogen bond donor) to 2.5 (strong acceptor). For many years it was believed that the correlation of Siamwiza et al. (1975) also applied to filamentous viruses containing tyrosine residues (Thomas et al., 1983). However, recent detailed studies of *Ff* filamentous viruses incorporating deuterated tyrosines, deuterated phenylalanines, and single-site mutations of the pVIII tyrosines demonstrate that neither Tyr^{21} nor Tyr^{24} in pVIII subunits of the *Ff* assembly exhibits the canonical tyrosine Fermi doublet (Overman et al., 1994; Overman and Thomas, 1995). Instead, these tyrosines are characterized by a singlet near 850–855 cm^{-1}. (The companion Raman band near 825–830 cm^{-1} in the Raman spectrum of *Ff* is due not to tyrosines but to phenylalanines of the pVIII subunit. This unexpected finding has also been demonstrated for tyrosines Tyr^{25} and Tyr^{40} of *Pf1* filamentous virus (A. Armstrong, S. A. Overman and G. J. Thomas, Jr., unpublished results).)

In the *Ff* assembly model of Fig. 5 *b*, one face of the aromatic ring of Tyr^{24} ($k = 0$) makes a close approach (~3 Å) to atoms of the same pVIII main chain in the direction of the N-terminus (ca. Tyr^{21} and Glu^{20}). Conversely, the opposite face is separated by more than 6 Å from its nearest neighbor (e.g., Asp^{12}, $k = -6$). Likewise, one face of the ring of Tyr^{21} ($k = 0$) is close to side-chain carbons of Leu^{41} ($k = 11$, not shown), but the opposite face has no near neighbors within 5.5 Å. Thus interactions involving π electrons of one face of the aromatic rings of Tyr^{21} and Tyr^{24} appear to be uncompensated by similar interactions on the opposing face. The unusual aromatic ring environment for each tyrosine may be a contributing factor in precluding Fermi resonance interaction involving ring modes near 840 and 420 cm^{-1}, and thus may account for the anomalous singlet marker band observed near 850 cm^{-1}.

Although the region 800–850 cm^{-1} of the Raman spectrum of *Ff* cannot currently be interpreted in terms of tyrosine phenoxyl hydrogen bonding, other Raman markers of OH interactions have been identified (Takeuchi et al., 1989). Of particular interest is the Raman band assigned to the exocyclic C-O stretching vibration (normal mode $\nu_{7a'}$), which occurs near 1265–1275 cm^{-1} for a phenoxyl OH donor, near 1230–1240 cm^{-1} for a phenoxyl OH acceptor, and near 1255 cm^{-1} for a phenoxyl OH group involved as both donor and acceptor (Takeuchi et al., 1989). Because the $\nu_{7a'}$ vibration is localized at the phenoxyl group, it may also be less sensitive to the aromatic ring environment than are ring vibrations of the 800–850 cm^{-1} region. Thus the correlation between $\nu_{7a'}$ and phenoxyl hydrogen bonding may be applicable to the tyrosines of filamentous viruses. Off-resonance Raman studies of wild-type *fd* and of the mutants *f1*(Y21M) and *f1*(Y24M) have shown that $\nu_{7a'}$ occurs at 1268 cm^{-1} for Tyr^{21} and at 1261 cm^{-1} for Tyr^{24} (Overman and Thomas, 1995). This implies that the phenolic OH group of Tyr^{21} is a hydrogen bond donor, whereas that of Tyr^{24} is both donor and acceptor. Interestingly, such hydrogen bonding roles for Tyr^{21} and Tyr^{24} are consistent with our proposed pVIII assembly model of Fig. 5 *b*, wherein the Tyr^{21} OH is hydrogen bonded to the Asp^4 CO_2^- group and the Tyr^{24} OH is hydrogen bonded to both Glu^{20} CO_2^- and Lys^8 NH_3^+ groups. Conversely, tyrosine hydrogen bonding partners in the original 1IFJ model (Fig. 5 *a*) are not consistent with the observed $\nu_{7a'}$ Raman marker bands.

Conformation and environment of Trp^{26}

The tryptophan residue (Trp^{26}) of pVIII exhibits unusual CD and Raman spectroscopic properties. For example, Arnold and co-workers (Arnold et al., 1992) have shown that the contribution of Trp^{26} to the far-UV CD spectrum of *fd* is unusual in both bandshape and amplitude. Similarly, the indole ring vibration $\omega 3$ (also referred to as W3), which is a measure of the absolute value of the $\chi^{2,1}$ torsion angle of the tryptophan side chain (Miura et al., 1989; Maruyama and Takeuchi, 1995), is unusually high in frequency (1560 ± 1 cm^{-1}) in both off-resonance Raman and UVRR spectra of *Ff* (Aubrey and Thomas, 1991; Takeuchi et al., 1996; Wen et al., 1997). This high $\omega 3$ frequency is confirmed in the present RLID spectra (Figs. 2 and 3). The usual frequency interval observed for $\omega 3$ in Raman spectra of globular proteins and indole model compounds is 1542–1557 cm^{-1}; this interval correlates with $|\chi^{2,1}|$ torsions in the range 60°-120° (Miura et al., 1989). It has also been noted that polarized Raman results (Tsuboi et al., 1996a) and standard rotamer libraries (Ponder and Richards, 1987) require a positive sign for $\chi^{2,1}$. Accordingly, in previous Raman studies (Aubrey and Thomas, 1991; Tsuboi et al., 1996a; Takeuchi et al., 1996), the *Ff* structure has been modeled assuming a $\chi^{2,1}$ of +120 ± 10°. The currently proposed structural model (Fig. 5 *b*) also incorporates a large positive value for $\chi^{2,1}$, viz., +127°.

It should be noted that the model of Fig. 5 *b* retains the phenylalanine ring packing originally suggested by Marvin and co-workers. As seen in Fig. 5, Phe^{42} ($k = 11$), Phe^{11} ($k = -6$), and Phe^{45} ($k = 11$) form a trio of stacked phenyl rings. If this arrangement is to be retained, as seems energetically favorable, a large positive value for $\chi^{2,1}$ of Trp^{26} is required to prevent a clash between the Cζ3 atom of Trp^{26} and the ring of Phe^{42}. The proximity of Trp^{26} to Phe^{42} may also help to stabilize the hydrophobic packing of phenyl rings and may well be a factor in determining the extraordinary CD signal (Arnold et al., 1992; Woody, 1994).

Miura et al. (1988) have demonstrated that the frequency of the indole $\omega 17$ Raman band is a marker of hydrogen bonding strength at the indole NH site. The $\omega 17$ frequency ranges from 883 cm^{-1} in the non-hydrogen-bonded state to 871 cm^{-1} in very strongly hydrogen-bonded states. In the off-resonance Raman spectrum of *fd*, the $\omega 17$ mode of Trp^{26} gives a band at 876 cm^{-1} (Aubrey and Thomas, 1991). Furthermore, the $\omega 17$ Raman band is invariant to Y21M and Y24M mutations (Overman and Thomas, 1995). Therefore, it has been concluded that the NH site of Trp^{26} is involved in a hydrogen bond of moderate strength (Aubrey and Thomas, 1991), and that this hydrogen bond does not in-

volve either Tyr^{21} or Tyr^{24} (Overman and Thomas, 1995). In the model proposed here (Fig. 5 *b*), the indole NH of Trp^{26} is not within apparent hydrogen bonding distance of any other side chain. It remains plausible that the indole NH of Trp^{26} is hydrogen bonded to solvent water, as suggested earlier (Aubrey and Thomas, 1991). It is well known that tryptophan residues exposed to solvent water exhibit $\omega 17$ near 877 cm^{-1} (Miura et al., 1988).

CONCLUSIONS

The angles of inclination of the phenolic twofold axes of Tyr^{21} and Tyr^{24} in the pVIII coat protein subunit of the *Ff* filamentous virus have been determined by the recently developed technique of ultraviolet Raman linear intensity difference spectroscopy. These are the first experimentally determined orientations of tyrosine phenolic moieties in a filamentous virus assembly. The orientation determined for the phenolic ring of Tyr^{21} is close to the value proposed in the x-ray fiber diffraction-based model of Marvin and coworkers (Protein Data Bank, identification code 1IFJ). On the other hand, the orientation determined for the phenolic ring of Tyr^{24} differs from that of the 1IFJ model by a rotation of $\sim 40°$ about the $C\alpha$-$C\beta$ bond. The present results have been combined with the recently determined orientation of the indole side chain of residue Trp^{26} (Takeuchi et al., 1996; Tsuboi et al., 1996a) and with the subunit main-chain conformation and packing symmetry of the 1IFJ assembly to develop a self-consistent model for the *Ff* virion. In the model proposed here, it is shown that aromatic ring environments and hydrogen bonding states of donor and acceptor groups of Tyr^{21}, Tyr^{24}, and Trp^{26} are consistent with all applicable correlations developed for Raman marker bands of these residues. The present model should serve as a basis for further refinement of the molecular architecture of the *Ff* virion assembly.

This work was supported by research grants from the Ministry of Education, Science and Culture of Japan (04640467 and 08874062 to HT) and the U.S. National Institutes of Health (GM50776 to GJT).

REFERENCES

Arnold, G. E., L. A. Day, and A. K. Dunker. 1992. Tryptophan contributions to the unusual circular dichroism of *fd* bacteriophage. *Biochemistry.* 31:7948–7956.

Aubrey, K. L., and G. J. Thomas, Jr. 1991. Raman spectroscopy of filamentous bacteriophage *Ff* (*fd, M13, f1*) incorporating specifically-deuterated alanine and tryptophan side chains. Assignments and structural interpretation. *Biophys. J.* 60:1337–1349.

Banner, D. W., C. Nave, and D. A. Marvin. 1981. Structure of the protein and DNA in *fd* filamentous bacterial virus. *Nature.* 289:814–817.

Bendet, I. J., and J. E. Mayfield. 1976. Ultraviolet dichroism of *fd* bacteriophage. *Biophys. J.* 7:111–119.

Bhattacharjee, S., M. J. Glucksman, and L. Makowski. 1992. Structural polymorphism correlated to surface charge in filamentous bacteriophages. *Biophys. J.* 61:725–735.

Clack, B. A., and D. M. Gray. 1989. A CD determination of the α-helix contents of the coat proteins of four filamentous bacteriophages: *fd*, *IKe*, *Pf1*, and *Pf3. Biopolymers.* 28:1861–1873.

Clack, B. A., and D. M. Gray. 1992. Flow linear dichroism spectra of four filamentous bacteriophages: DNA and coat protein contributions. *Biopolymers.* 32:795–810.

Cross, T. A., and S. J. Opella. 1985. Protein structure by solid state nuclear magnetic resonance. Residues 40 to 45 of bacteriophage *fd* coat protein. *J. Mol. Biol.* 182:367–381.

Cross, T. A., P. Tsang, and S. J. Opella. 1983. Comparison of protein and deoxyribonucleic acid backbone structures in *fd* and *Pf1* bacteriophages. *Biochemistry.* 22:721–726.

Day, L. A., C. J. Marzec, S. A. Reisberg, and A. Casadevall. 1988. DNA packing in filamentous bacteriophages. *Annu. Rev. Biophys. Biophys. Chem.* 17:509–539.

Denhardt, D. T., D. Dressler, and S. Ray, editors. 1978. The Single Stranded DNA Phages. Cold Spring Harbor Laboratory, Cold Spring Harbor, NY.

Fritzsche, H., T. A. Cross, S. J. Opella, and N. R. Kallenbach. 1981. Structure and architecture of the bacterial virus *fd*. An infrared linear dichroism study. *Biophys. Chem.* 14:283–291.

Glucksman, M. J., S. Bhattacharjee, and L. Makowski. 1992. Three-dimensional structure of a cloning vector. X-ray diffraction studies of filamentous bacteriophage *M13* at 7 Å resolution. *J. Mol. Biol.* 226: 455–470.

Makowski, L., and D. L. D. Caspar. 1981. The symmetries of filamentous phage particles. *J. Mol. Biol.* 145:611–617.

Maruyama, T., and H. Takeuchi. 1995. Effects of hydrogen bonding and side-chain conformation on the Raman bands of tryptophan-2,4,5,6,7-d_5. *J. Raman Spectrosc.* 26:319–324.

Marvin, D. A. 1990. Model-building studies of *Inovirus.* Genetic variations on a geometric theme. *Int. J. Biol. Macromol.* 12:125–138.

Marvin, D. A., R. D. Hale, C. Nave, and M. Helmer Citterich. 1994. Molecular models and structural comparison of native and mutant class I filamentous bacteriophages, *Ff* (*fd*, *f1*, *M13*), *If1* and *IKe. J. Mol. Biol.* 235:260–286.

Marvin, D. A., W. J. Pigram, R. L. Wiseman, E. J. Wachtel, and F. J. Marvin. 1974. Filamentous bacterial viruses. XII. Molecular architecture of the class I (*fd*, *If1*, *IKe*) virion. *J. Mol. Biol.* 88:581–600.

Marvin, D. A., and E. J. Wachtel. 1975. Structure and assembly of filamentous bacterial viruses. *Nature.* 253:19–23.

Marvin, D. A., and E. J. Wachtel. 1976. Structure and assembly of filamentous bacterial viruses. *Philos. Trans. R. Soc. Lond. Biol.* 276: 81–98.

Marzec, C. J., and L. A. Day. 1988. A theory of the symmetries of filamentous bacteriophages. *Biophys. J.* 53:425–440.

McGregor, M. J., S. A. Islam, and M. J. E. Sternberg. 1987. Analysis of the relationships between side-chain conformation and secondary structure in globular proteins. *J. Mol. Biol.* 198:295–310.

Miura, T., H. Takeuchi, and I. Harada. 1988. Characterization of individual tryptophan side chains in proteins using Raman spectroscopy and hydrogen deuterium exchange kinetics. *Biochemistry.* 27:88–94.

Miura, T., H. Takeuchi, and I. Harada. 1989. Tryptophan Raman bands sensitive to hydrogen bonding and side-chain conformation. *J. Raman Spectrosc.* 20:667–671.

Opella, S. J., T. A. Cross, J. A. DiVerdi, and C. F. Sturm. 1980. Nuclear magnetic resonance of the filamentous bacteriophage *fd. Biophys. J.* 80:531–548.

Opella, S. J., P. L. Stewart, and K. G. Valentine. 1987. Protein structure by solid-state NMR spectroscopy. *Q. Rev. Biophys.* 19:7–49.

Overman, S. A., K. L. Aubrey, N. S. Vispo, G. Cesareni, and G. J. Thomas, Jr. 1994. Novel tyrosine markers in Raman spectra of wild-type and mutant (Y21M and Y24M) *Ff* virions indicate unusual environments for coat protein phenoxyls. *Biochemistry.* 33:1037–1042.

Overman, S. A., and G. J. Thomas, Jr. 1995. Raman spectroscopy of the filamentous virus *Ff* (*fd*, *f1*, *M13*). Structural interpretation for coat protein aromatics. *Biochemistry.* 34:5440–5451.

Overman, S. A., M. Tsuboi, and G. J. Thomas, Jr. 1996. Subunit orientation in the filamentous virus *Ff* (*fd, f1, M13*). *J. Mol. Biol.* 259:331–336.

Ponder, J. W., and F. M. Richards. 1987. Tertiary templates for proteins. Use of packing criteria in the enumeration of allowed sequences for different structural classes. *J. Mol. Biol.* 193:775–791.

Siamwiza, M. N., R. C. Lord, M. C. Chen, T. Takamatsu, I. Harada, H. Matsuura, and T. Shimanouchi. 1975. Interpretation of the doublet at 850 and 830 cm^{-1} in the Raman spectra of tyrosyl residues in proteins and certain model compounds. *Biochemistry.* 14:4870–4876.

Symmons, M. F., L. C. Welsh, C. Nave, D. A. Marvin, and R. N. Perham. 1995. Matching electrostatic charge between DNA and coat protein in filamentous bacteriophage. Fibre diffraction of charge-deletion mutants. *J. Mol. Biol.* 245:86–91.

Takeuchi, H., M. Matsuno, S. A. Overman, and G. J. Thomas, Jr. 1996. Raman linear intensity difference of flow-oriented macromolecules. Orientation of the indole ring of tryptophan-26 in filamentous virus *fd*. *J. Am. Chem. Soc.* 118:3498–3507.

Takeuchi, H., N. Watanabe, Y. Satoh, and I. Harada. 1989. Effects of hydrogen bonding on the tyrosine Raman bands in the 1300–1150 cm^{-1} region. *J. Raman Spectrosc.* 20:233–237.

Thomas, G. J., Jr. 1985. Resolution enhancement in Raman spectra of biological macromolecules by Fourier deconvolution. Applications to single-stranded DNA and RNA viruses. *Spectrochim. Acta.* 41A: 217–221.

Thomas, G. J., Jr., and P. Murphy. 1975. Structure of coat proteins in *Pf1* and *fd* virions by laser Raman spectroscopy. *Science.* 188:1205–1207.

Thomas, G. J., Jr., B. Prescott, and L. A. Day. 1983. Structure similarity, difference and variability in the filamentous viruses *fd*, *If1*, *IKe*, *Pf1*, and *Xf*. Investigation by laser Raman spectroscopy. *J. Mol. Biol.* 165: 321–356.

Tsuboi, M., S. A. Overman, and G. J. Thomas, Jr. 1996a. Orientation of tryptophan-26 in coat protein subunits of the filamentous virus *Ff* by polarized Raman microspectroscopy. *Biochemistry*. 35: 10403–10410.

Tsuboi, M., T. Ueda, K. Ushizawa, Y. Ezaki, S. A. Overman, and G. J. Thomas, Jr. 1996b. Raman tensors for the tryptophan side chain in proteins determined by polarized Raman microspectroscopy of oriented *N*-acetyl-L-tryptophan crystals. *J. Mol. Struct.* 379:43–50.

Wachtel, E. J., R. L. Wiseman, W. J. Pigram, D. A. Marvin, and L. Manuelidis. 1974. Filamentous bacterial viruses. XIII. Molecular structure of the virion in projection. *J. Mol. Biol.* 88:601–618.

Webster, R. E. 1996. Biology of the filamentous bacteriophage. *In* Phage Display of Peptides and Proteins. B. K. Kay, J. Winter, and J. McCafferty, editors. Academic Press, London. 1–20.

Wen, Z. Q., S. A. Overman, and G. J. Thomas, Jr. 1997. Structure and interactions of the single-stranded DNA genome of filamentous virus *fd*. Investigation by ultraviolet resonance Raman spectroscopy. *Biochemistry.* 36:7810–7820.

Williams, R. W., A. K. Dunker, and W. L. Peticolas. 1984. Raman spectroscopy and deuterium exchange of the filamentous phage *fd*. *Biochim. Biophys. Acta.* 791:131–144.

Williams, K. A., M. Glibowicka, L. Zuomei, L. Hong, A. R. Khan, Y. M. Y. Chen, J. Wang, D. A. Marvin, and C. M. Deber. 1995. Packing of coat protein amphipathic and transmembrane helices in filamentous bacteriophage *M13*. Role of small residues in protein oligomerization. *J. Mol. Biol.* 252:6–14.

Woody, R. W. 1994. Contributions of tryptophan side chains to the far-ultraviolet circular dichroism of proteins. *Eur. Biophys. J.* 23: 253–262.